Gastrointestinal Segment Tracking of Ingestible Capsules Using Biodegradable Superstrates

Azar Hadi*, Erdem Cil†‡, Zeliha Cansu Canbek Ozdil§, Denys Nikolayev†, and Sema Dumanli*
*Electrical and Electronics Engineering Dept., Bogazici University, Turkey
†IETR UMR 6164, CNRS / Univ. Rennes, France
‡BodyCAP, Hérouville-Saint-Clair, France
§Yeditepe University, Turkey
sema.dumanli@boun.edu.tr

***Abstract*—Miniaturized wireless capsule endoscopes offer minimally invasive real-time monitoring of vital parameters of the gastrointestinal tract. Although various ingestible capsules are commercially available for wireless endoscopy, the precise real-time localization of these capsules within the tract remains a challenge. This work proposes the utilization of a pH-sensitive biodegradable superstrate for gastrointestinal segment tracking in the 433 MHz Industrial, Scientific, and Medical (ISM) band. The superstrate consists of three rings engineered to degrade at specific pH levels that correspond to the distinct environments of the GI tissues – stomach, small intestine, and large intestine. This superstrate covers the outer surface of a capsule which features an integrated conformal dipole antenna. Hence, biodegradation of each ring of the superstrate in its respective GI segment leads to the alteration of the near-field of the antenna, changing its center frequency and reflection coefficient at 434 MHz in each segment. In this way, biodegradation process links the location data to the input parameters of the antenna, enabling segment tracking within the tract. Simulation results show that a shift of at least 5 MHz can be created in the center frequency as the capsule advances along each segment while the antenna is kept operational over the 433 MHz ISM band throughout the entire tract. Finally, preliminary tests using liquid gastrointestinal phantoms are conducted to validate the proposed technique.**

***Index Terms*—biodegradable materials, implant antenna, ingestible capsule, pH sensors, wireless bioelectronics.**

I. Introduction

Recent advancements in bioelectronics have led to the development of ingestible wireless medical devices that have significantly improved the methods used in current health applications [1]–[3]. Among these devices, wireless capsule endoscopes (WCE) enable healthcare professionals to monitor different segments of the gastrointestinal (GI) tract that are unreachable or difficult to reach through other endoscopy procedures [4]. An open challenge for the capsule technology is the real-time localization of the capsule within the tract. The position information can be beneficial for various purposes such as detecting the exact location of an abnormality or facilitating in-situ drug delivery [5].

To locate a capsule in the GI tract, multiple solutions have been proposed in the literature under three main categories: video-based [6], radio frequency (RF)-based [7], and magnetic field-based localization [8]. Although these methods are a step forward to tackling this challenge, they require additional on-body and in-body components to be integrated into the system. In this paper, we propose a simple solution that can be added on to an existing platform for tracking the position of the capsule inside the GI tract.

Antenna design for ingestible capsules has challenges that are unique to the nature of the communication path [9]. One of these challenges is the detuning of the input impedance due to the varying surrounding environment as the capsule advances in the GI tract. The capsule is exposed to the stomach, small intestine, and large intestine of which electromagnetic (EM) properties (relative permittivity, ε_r, and electrical conductivity, σ) and chemical properties (pH) vary [10]. Although a number of studies propose antenna designs that are immune to the EM changes through the GI tract [11]–[13], Cil et. al. have proposed to make use of this variation for capsule localization in the GI tract [14]. Specifically, they demonstrated that the differences in the EM properties of the tissues changed the reflection coefficient of the antenna which then was related to the current location of the capsule. In this paper, an improvement to this technique is proposed which aims to utilize the differences in chemical properties in addition to the EM properties. For this purpose, the capsule presented in [14] is coated with three rings of pH sensitive biodegradable superstrate that degrade in different segments of the GI tract. In this way, degradation of the rings contributes to the detuning of the ingestible antenna observed in each segment, thereby facilitating the segment tracking. Although biodegradation of resonating structures under different pH conditions has previously been used for various wireless sensing purposes such pH sensing [15], [16], this paper offers using biodegradation for GI segment tracking for the first time in the literature.

This paper is organized as follows. Section II demonstrates the ingestible capsule model along with the simulation setup used in this work and discusses the simulation results. Section III presents the method to fabricate the biodegradable superstrate for prototyping and preparation of the measurement setup. Section IV shares the measurement results. Finally, Section V concludes the work.

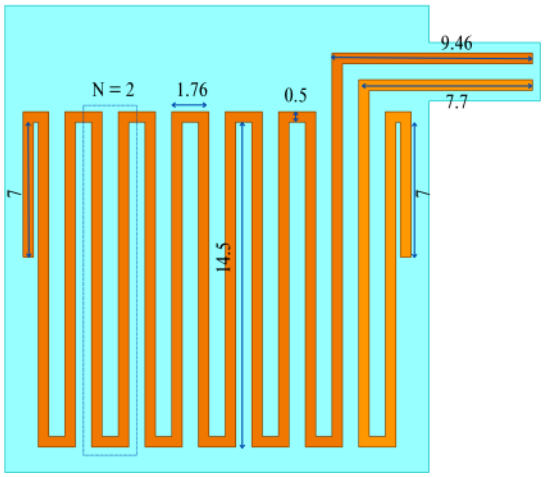

Fig. 1. Optimized dimensions of the meandered conformal dipole antenna operating at 433 MHz in the phantom with time-averaged EM properties of the GI tract (units: mm).

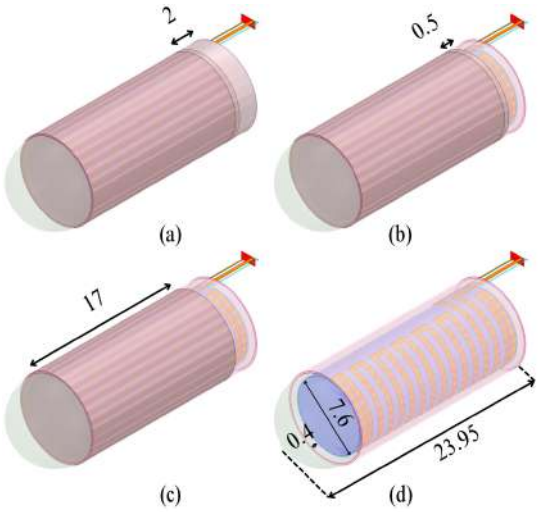

Fig. 2. Capsule model and three consecutive degradation steps in different GI tissues (units: mm). (a) Initial (without any degradation). (b) Stomach. (c) Small intestine. (d) Large intestine.

II. Capsule Model and Simulations

A. Capsule Model and Simulation Setup

To investigate the method proposed here, the capsule-integrated antenna that was previously designed by the authors is used [14]. This antenna is an offset-fed meandered dipole antenna designed on a 0.1 mm-thick Rogers CLTE-MW substrate (ε_r = 2.97). It conforms to the inner surface of a (24×⌀8.4) mm biocompatible polylactic-acid (PLA, $\varepsilon_r = 2.7$, $\delta = 0.003$) capsule with an encapsulation thickness of 0.4 mm. The antenna is optimized to operate in the 433 MHz Industrial, Scientific, and Medical (ISM) band in the middle of a (120×⌀100) mm cylindrical homogeneous phantom. The phantom has the time-averaged EM properties of the GI tissues ($\varepsilon_r = 63$, $\sigma = 1.02$ S/m at 434 MHz, see [17]). The optimized dimensions of the antenna can be seen in Fig. 1.

For the study presented in this paper, the capsule with the conformal dipole antenna is coated with three rings of 0.15 mm-thick biodegradable film (ε_r = 5), each disintegrating at different pH levels. The degradation is modelled as seen in Fig 2. The degradation of the biodegradable superstrate increases the effective permittivity of the antenna and results in a shift in its center frequency. The rings are designed such that this shift is in at least 5 MHz steps. The width of the first ring that is expected to degrade in the stomach is optimized inside a stomach phantom (ε_r = 67.2, σ = 1.01 S/m, 434 MHz) of the same size as the time-averaged GI phantom. Similarly, the width of the second ring and the third ring are optimized inside a small intestine (ε_r = 65.3, σ = 1.92 S/m, 434 MHz) and a large intestine phantom (ε_r = 62, σ = 0.87 S/m, 434 MHz), respectively. The optimized widths of the rings can be seen in Fig. 2.

B. Simulation Results

Fig. 3a and Fig. 3b show the simulated magnitude and phase response of the antenna, respectively, in the initial state and in three GI tissues. The center frequency (f_c) of the antenna for each case and the magnitude and the phase of the reflection at these center frequencies are tabulated in Table I. In addition, Table I also shows the simulated magnitude and phase values at 434 MHz.

TABLE I
Simulated Center Frequency of the Antenna and Magnitude and Phase of the Reflection Coefficient at Corresponding Center Frequencies as well as at 434 MHz for Different Degradation Steps

Deg. Step	f_c (MHz)	$f = f_c$ $\lvert S_{11}\rvert$ (dB)	$f = f_c$ $\angle S_{11}$ (deg.)	f = 434 MHz $\lvert S_{11}\rvert$ (dB)	f = 434 MHz $\angle S_{11}$ (deg.)
Initial	446	−16.7	156.5	−10.8	−128.4
Stomach	440	−13.9	158	−12.4	−163
Small Int.	430	−15.4	155.5	−14.6	125.5
Large Int.	425	−17.8	153	−13.1	87.1

As can be seen from Table I, a shift of at least 5 MHz in the center frequency of the antenna is observed at each degradation step. Moreover, the magnitude and phase at 434 MHz change notably at each step. Therefore, it can be stated that the degradation of the coating leads to changes in the magnitude and phase response of the antenna that are sufficiently large to track the location of the capsule in the GI tract, thereby validating the feasibility of the proposed technique. Similar to the results presented in [14], the phase values change in larger intervals than the magnitude values. This result indicates that it is more suitable to follow the changes in the phase for GI segment tracking. Finally, it can be observed that the antenna has a reasonable impedance matching ($\lvert S_{11}\rvert <$ -10 dB) for the entire 433 MHz ISM band at each degradation step. This demonstrates that the proposed technique does not intercept the normal operation of the capsule.

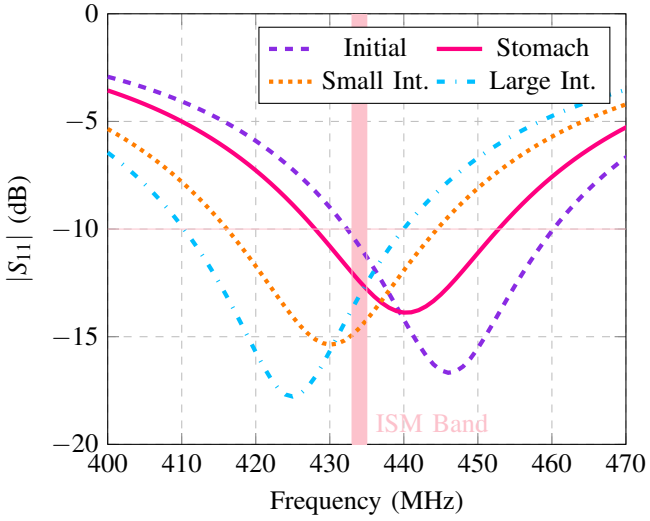

(a)

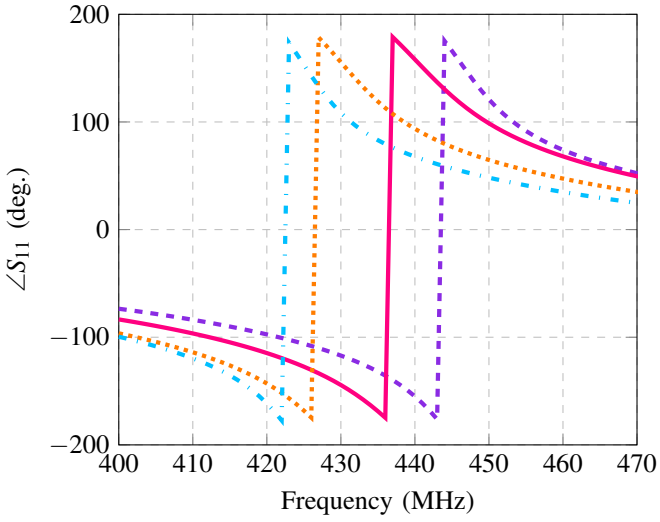

(b)

Fig. 3. Simulated reflection coefficients for different degradation steps: (a) Magnitude. (b) Phase.

III. Prototyping and Measurement Setup

A. Prototyping

A prototype of the model described in Section II-A is prepared for the measurements. For the capsule, the prototype presented in [14] is used. This prototype consists of the dipole antenna fabricated with laser ablation technique, the capsule model fabricated with 3D-printing, a coaxial cable for electrical connection, an epoxy-resin cover around antenna-cable connection as a watertight seal, and ferrite rings covering the antenna end of the coaxial cable. Ferrite rings were used to eliminate the effect of the environment surrounding the cable on the operation of the antenna. Although the use of the ferrite rings does not eliminate the effect of the cable on the operation of the antenna, they stabilize this cable-effect in different GI segments by making it independent of the environment around the cable. This ensures that the changes in the antenna parameters result from the changes in the environment around the antenna and not from those around the cable [18].

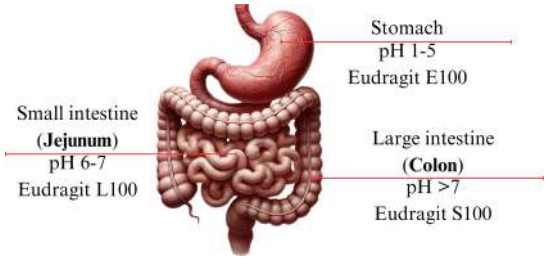

Fig. 4. The chemical properties of the tissues in the human GI tract and the corresponding Eudragit grades.

As for the superstrate covering the capsule, thin films based on Eudragit formulations, specifically designed to degrade at different pH levels (E100, L100, and S100) are used. The intrinsic pH gradients present within the GI tract as seen in Fig. 4 cause the site-specific degradation of the films forming the superstrate. Each film comprises a distinct Eudragit formulation, carefully engineered to degrade at predetermined pH levels that correspond to the varying environments of the GI tract: the stomach, the small intestine, and the large intestine. Eudragit E100 is designed to dissolve at the low pH found in the stomach (pH 1-5), ensuring immediate degradation in highly acidic environment. The Eudragit L100 dissolves in a slightly acidic environment, at a pH above 5.5, aligning with the conditions in the small intestine. Finally, Eudragit S100 dissolves at pH levels above 7.0, which corresponds to the chemical environment of the large intestine.

To realize the superstrate on the outer wall of the capsule, the capsule is coated with polymer solutions prepared in a solvent mixture consisting of 60% acetone and 40% isopropyl alcohol. The S100 and L100 polymers are formulated at a concentration of 25 wt.%, while E100 is prepared at 50 wt.%. To achieve selective coating, the ends of the capsule are masked using parafilm, and a 2.5 cm section is masked with label paper. The polymer layers are applied using a dip-coating device operated at a controlled speed of 150 mm/min. Once the coating dried, the mask is carefully removed by making precise incisions at the mask boundary with a snap blade knife. The capsule coated with this methodology can be seen in Fig. 5 (a). Note that the width of the each film is equal to the width of the corresponding ring in the numerical study presented in Section II-A.

B. Measurement Setup

The measurements are conducted in liquid electrochemical phantoms replicating EM properties and pH values of the stomach, small intestine, and large intestine. These phantoms are developed using water, sugar, salt, citric acid, and sodium hydroxide (NaOH). Table II tabulates the amount of each ingredient used for the fabrication. First, sugar and salt are added to water to reach the target relative permittivity and

TABLE II
REQUIRED AMOUNT OF EACH INGREDIENT USED TO PREPARE THE TISSUE-MIMICKING PHANTOMS AND MEASURED EM PROPERTIES AND PH VALUES OF THE PHANTOMS

GI Segment	Water (g)	Sugar (g)	Salt (g)	Citric acid (mg)	NaOH (mg)	ε_r	σ	pH
Stomach	68.5	30.4	1.1	120	0	67.4	1.01	3
Small Int.	67	30.5	2.5	0	0	65.3	2	6.8
Large Int.	71	27.5	1.5	0	0.1	62.4	0.89	8.4

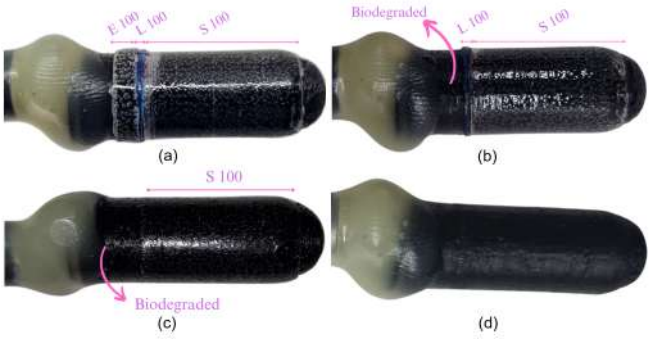

Fig. 5. Capsule coated with three films forming the superstrate and the degradation steps in the measurements. (a) Prepared prototype with the superstrate before any degradation. Degradation in the (b) stomach phantom, (c) small intestine phantom, and (d) large intestine phantom.

conductivity values, respectively. The EM properties of the mixtures are measured using a SPEAG DAK-3.5 probe [19] and tabulated in Table II. Next, citric acid and sodium hydroxide are added to adjust the pH values, and the pH of the final mixtures are measured using an Isolab portable pH meter [20] (Table II). Note that the effect of citric acid and sodium hydroxide on the EM properties is negligible. Finally, for every 1000 g phantom, 0.3 g of sodium azide is added to inhibit bacterial growth. For the measurements, the prototype is placed inside the prepared phantoms one by one as visualized in Fig. 6 with the stomach phantom.

IV. MEASUREMENT RESULTS

Fig. 5 (b)–(d) show the step-by-step degradation of the superstrate in different GI phantoms. As can be seen, in line with the objective, the three films degrade in their respective GI segments, confirming the effectiveness of the method used to prototype the superstrate. Moreover, Fig. 7a and Fig. 7b show the measured magnitude and phase of the reflection coefficient at every degradation step, respectively. Table III tabulates the center frequency of the antenna at every degradation step as well as the magnitude and phase of the reflection coefficient at these frequencies. From the results, it can be seen that the center frequency of the prototype before degradation is shifted to 384 MHz due to the effect of the cable. Furthermore, it is observed that the center frequency shifts by 40 MHz from the small intestine to the large intestine; however, it remains unchanged for

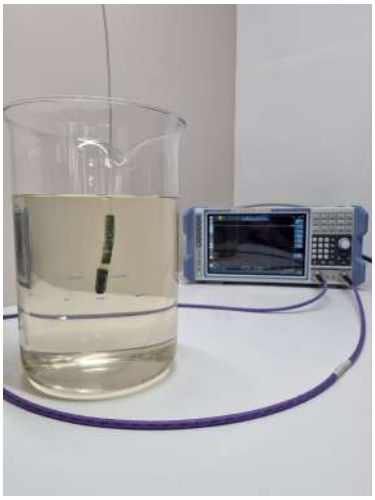

Fig. 6. Prototype placed in the prepared stomach phantom for measurements.

TABLE III
MEASURED CENTER FREQUENCY OF THE ANTENNA FOR DIFFERENT DEGRADATION STEPS AND THE MAGNITUDE AND PHASE OF THE REFLECTION COEFFICIENT AT THESE CENTER FREQUENCIES

Degradation Step	f_c (MHz)	$\lvert S_{11}\rvert$ (dB)	$\angle S_{11}$ (deg.)
Initial	384	-19.3	137.2
Stomach	384	-19	138.5
Small Intestine	384	-19.4	140
Large Intestine	344	-15.3	-84

the the other degradation steps. This disagreement with the simulation results arises from two facts. Firstly, simulations use an approximate relative permittivity value (ε_r = 5) for the three films forming the superstrate. However, the relative permittivity values of the manufactured films may vary, and it is challenging to determine the real values as the films are ultra-thin. Consequently, the differences in the relative permittivity values lead to the disagreement between the results. Secondly, during the prototyping, we have a limited control on the thickness of the coating. Hence, the real thickness could differ from the one implemented in the simulations (0.15 mm), contributing to the observed disagreement. Nevertheless, the 40 MHz shift observed from the initial state to the large intestine proves the feasibility of the proposed method. The preliminary measurement results obtained in this paper are open to improvement, which defines our future work.

V. CONCLUSION

A method to improve the effectiveness of the use of antenna impedance detuning for GI segment tracking of ingestible capsules is studied in this work. It has been shown that the change in the input response of the capsule antenna as it advances through the GI tract can be engineered using a pH sensitive biodegradable superstrate. As each part of the superstrate degrades in a different segment depending on the acidity level, a shift of at least 5 MHz is introduced to the

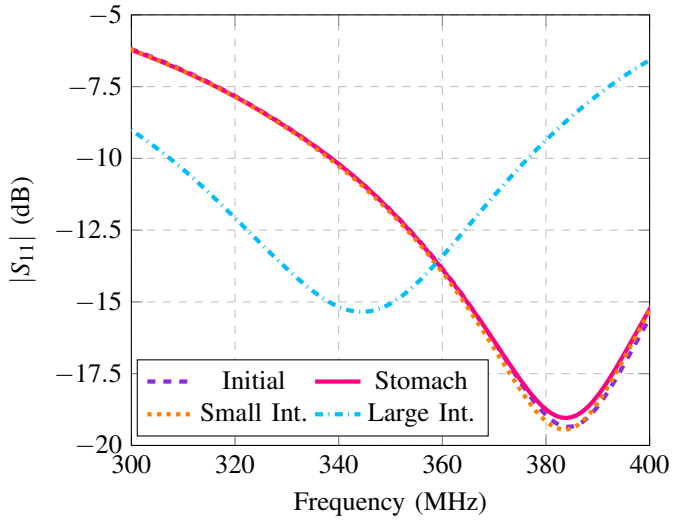

(a)

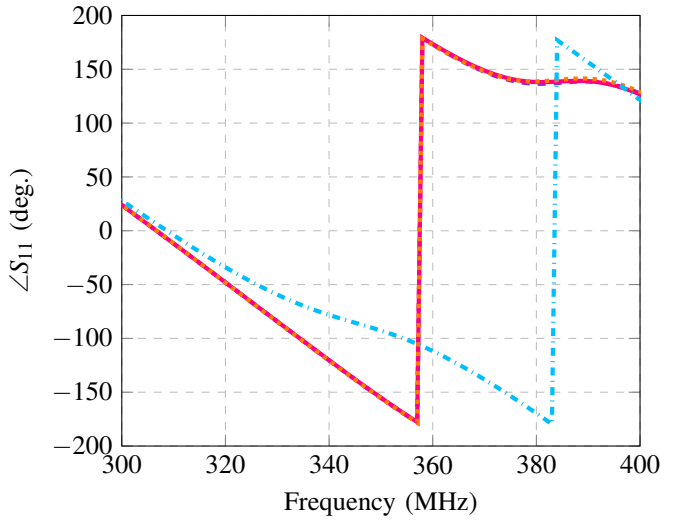

(b)

Fig. 7. Measured reflection coefficients at different degradation steps. (a) Magnitude. (b) Phase.

center frequency of the capsule antenna in each segment, enabling the localization of the capsule inside the tract. Moreover, the antenna remains operational in the 433 MHz ISM band throughout the GI tract, which proves that the proposed method does not interfere with the existing wireless link. Our future work aims at EM characterization of the ultra-thin films used in the prototyping of the superstrate for an improved design and measurements.

ACKNOWLEDGMENT

This work was supported in part by the French *Agence Nationale de la Recherche* (ANR) under grant ANR-21-CE19-0045 (project "MedWave"), in part by Région Bretagne (France) through the *Stratégie d'attractivité durable* (SAD) project "EM-NEURO", in part by the BodyCAP Company, and in part by the European Regional Development Fund (ERDF) and Région Normandie (France).

REFERENCES

[1] Y. Rahmat-Samii and L. Song, "Advances in communication and biomedical antenna developments at the UCLA antenna lab: Handheld, wearable, ingestible, and implantable [Bioelectromagnetics]," in IEEE Antennas and Propagation Magazine, vol. 63, no. 5, pp. 102-115, Oct. 2021.

[2] C. Steiger, A. Abramson, P. Nadeau, A. P. Chandrakasan, R. Langer, and G. Traverso, "Ingestible electronics for diagnostics and therapy," Nat. Rev. Mater., vol. 4, no. 2, pp. 83–98, Feb. 2019.

[3] D. Nikolayev, M. Zhadobov, R. Sauleau, and P. Karban, "Advances in body-centric wireless communication: Applications and state-of-the-art," IET, pp. 143–186, 2016.

[4] A. Kiourti and K. S. Nikita, "A review of in-Body biotelemetry devices: Implantables, ingestibles, and injectables," in IEEE Transactions on Biomedical Engineering, vol. 64, no. 7, pp. 1422-1430, July 2017.

[5] H. Mateen, R. Basar, A. U. Ahmed and M. Y. Ahmad, "Localization of wireless capsule endoscope: A systematic review," *IEEE Sensors Journal*, vol. 17, no. 5, pp. 1197-1206, 1 March 1, 2017.

[6] S. Zeising, A. S. Thalmayer, M. Lübke, G. Fischer and J. Kirchner, "Localization of passively guided capsule endoscopes—A review," *IEEE Sensors Journal*, vol. 22, no. 21, pp. 20138-20155, 1 Nov.1, 2022.

[7] M. Barbi, C. Garcia-Pardo, A. Nevarez, V. Pons Beltran, and N. Cardona, "UWB RSS-based localization for capsule endoscopy using a multilayer phantom and in vivo measurements," *IEEE Transactions on Antennas and Propagation*, vol. 67, no. 8, pp. 5035–5043, Aug. 2019.

[8] S. Zeising, K. Ararat, A. Thalmayer, D. Anzai, G. Fischer, and J. Kirchner, "Systematic performance evaluation of a novel optimized differential localization method for capsule endoscopes," *Sensors*, vol. 21, no. 9, p. 3180, May 2021.

[9] A. K. Skrivervik, M. Bosiljevac and Z. Sipus, "Fundamental limits for implanted antennas: Maximum power density reaching free space," in IEEE Transactions on Antennas and Propagation, vol. 67, no. 8, pp. 4978-4988, Aug. 2019.

[10] Gabriel S, Lau RW, Gabriel C. The dielectric properties of biological tissues: II. Measurements in the frequency range 10 Hz to 20 GHz. Phys Med Biol. 1996 Nov;41(11):2251-69.

[11] Z. Bao, Y. -X. Guo and R. Mittra, "An ultrawideband conformal capsule antenna with stable impedance matching," in IEEE Transactions on Antennas and Propagation, vol. 65, no. 10, pp. 5086-5094, Oct. 2017.

[12] M. K. Magill, G. A. Conway and W. G. Scanlon, "Tissue-independent implantable antenna for in-body communications at 2.36–2.5 GHz," in IEEE Transactions on Antennas and Propagation, vol. 65, no. 9, pp. 4406-4417, Sept. 2017.

[13] D. Nikolayev, M. Zhadobov, L. Le Coq, P. Karban and R. Sauleau, "Robust ultraminiature capsule antenna for ingestible and implantable applications," in IEEE Transactions on Antennas and Propagation, vol. 65, no. 11, pp. 6107-6119, Nov. 2017.

[14] E. Cil et al., "On the use of impedance detuning for gastrointestinal segment tracking of ingestible capsules," *IEEE Transactions on Antennas and Propagation*, vol. 71, no. 2, pp. 1977-1981, Feb. 2023.

[15] K. Ararat, O. Altan, S. Serbest, O. Baser and S. Dumanli, "A biodegradable implant antenna detecting post-surgical infection," *2020 14th European Conference on Antennas and Propagation (EuCAP)*, Copenhagen, Denmark, 2020, pp. 1-4.

[16] J. M. Rigelsford, B. F. Al-Azzawi, C. J. Davenport, and P. Novodvorsky, "A passive biodegradable implant for subcutaneous soft-tissue trauma monitoring," *IEEE journal of biomedical and health informatics*, vol. 19, no. 3, pp. 901–909, 2015.

[17] E. Cil, S. Dumanli and D. Nikolayev, "Examination of impedance response of capsule-integrated antennas through gastrointestinal tract," 2022 16th European Conference on Antennas and Propagation (EuCAP), Madrid, Spain, 2022, pp. 1-5.

[18] Y. L. Chang, and Q. X. Chu, "Ferrite-loaded dual-polarized antenna for decoupling of multiband multiarray antennas," IEEE Trans. Antennas Propag., vol. 69, no. 11, pp. 7419-7426, 2021.

[19] SPEAG DAK 3.5, [Online], October 2024, Available at https://speag.swiss/products/dak/dak-probes/.

[20] Isolab Laboratory Equipments, [Online], October 2024, Available at https://www.isolab.de/default.